Malaysian Applied Biology (2024) 53(3): 147-158
https://doi.org/10.55230/mabjournal.v53i3.2880

Research

Identification and Characterization of *Botrytis cinerea* Causing Gray Mold on Tomatoes in Cameron Highlands, Malaysia

Siti Fairuz Yusoff[1]*, Siti Izera Ismail[2], Farah Farhanah Haron[3], Zahir Shah Safari[4], Rohasmizah Hashim[5], Paiman[6]

1. Agricultural Science Department, Faculty of Technical and Vocational, Universiti Pendidikan Sultan Idris, 35900, Tanjong Malim, Perak, Malaysia
2. Department of Plant Protection, Faculty of Agriculture, Universiti Putra Malaysia, 43400 Serdang, Selangor, Malaysia
3. Biological Control Programme, Agrobiodiversity and Environment Research Centre, Malaysian Agricultural Research and Development Institute, 43400 Serdang, Selangor, Malaysia
4. Institute of Horticultural Production Systems, Vegetable Systems Modelling Section, Leibniz University Hannover, 30419 Hannover, Germany
5. Food Technology Department, Faculty of Applied Science, Universiti Teknologi MARA (UiTM), Kuala Pilah Campus, Pekan Parit Tinggi, 72000, Kuala Pilah, Negeri Sembilan, Malaysia
6. Department of Agrotechnology, Faculty of Agriculture, Universitas PGRI Yogyakarta, Yogyakarta 55182, Indonesia

*Corresponding author: yuezyusoff@gmail.com

ABSTRACT

Botrytis cinerea, commonly known as gray mold, is a pervasive fungal pathogen that affects a wide range of plant species, leading to significant agricultural losses. The identification of *Botrytis cinerea* in Malaysia is crucial for protecting the agricultural sector, minimizing economic losses, ensuring food security, maintaining export quality, addressing environmental concerns, and advancing scientific research. In the present research, tomato fruits collected from Cameron Highlands, Pahang, Malaysia showed gray mold disease symptoms of *B. cinerea*. The fungal isolates were examined morphologically for colony colour, growth rate, conidiophores, conidia shape, and sclerotia on PDA and V8 agar. According to the results, conidiophores appeared in grape shape and length was range of 21.26-32.52 µm, ovoid conidial dimensions were in the range of 10.03-16.08 × 7.37-11.15 µm and sclerotia size was range 1.91-4.50 × 1.70-4.00 mm. All isolates were attributed to the morphospecies *Botrytis cinerea* on account of these characteristics. The resulting sequences deposited in GenBank were accessions MT012053 to MT012062, respectively. A BLAST analysis of the resulting 550-bp nucleotide sequences showed 99-100% identity closest matched to *B. cinerea*. The pathogenicity experiments showed P6 isolates of *B. cinerea* were highly pathogenic and caused gray mold development on tomato fruits that led to severe symptoms in five days. Meanwhile, the least pathogenic isolate was P9. In terms of temperature, *B. cinerea* grew faster on PDA at 20ºC, slower grew below 20ºC and did not grow at 25ºC. Identification and characterization of *B. cinerea* on tomato could potentially provide information to assist disease management strategies for *B. cinerea*.

Key words: *Botrytis cinerea*, gray mold, *Lycopersicon esculentum* Mill, pathogenicity, tomato

Article History
Accepted: 3 August 2024
First version online: 30 September 2024

Cite This Article:
Yusoff, S.F., Ismail, S.I., Haron, F.F., Safari, Z.S., Hashim, R. & Paiman. 2024. Identification and characterization of Botrytis cinerea causing gray mold on tomatoes in Cameron Highlands, Malaysia. Malaysian Applied Biology, 53(3): 147-158. https://doi.org/10.55230/mabjournal.v53i3.2880

INTRODUCTION

Botrytis cinerea (teleomorph *Botryotinia fuckeliana*) is a causal agent of gray mold disease that infects a wide range of plant species, including tomatoes. As a destructive filamentous fungal pathogen, it results in severe damage to fresh commodities. Infections of *B. cinerea*, which cause postharvest decay, usually occur before harvest at the field level and remain latent until storage. Bautista-Banos (2014) explained that at the beginning of infections, a darker circular area is noticeable where the fruit tissues are more delicate than the other parts. Subsequently, abundant sporulation may appear, ranging from white to gray. Weak tissue, especially the wounded area, is vulnerable to infection. In a study by Leyronas *et al.* (2015), spore germination of this fungus was found to be aggressive in low temperatures with

high relative humidity. On the infected tissue surface, abundant conidia are produced and widely spread through wind dispersion. Thus, due to this nature, this pathogen is more easily able to infect other fruits within packaging boxes in cold storage.

Previous studies reported that the mycelium of *B. cinerea* is branched, septate, and varies in color from hyaline to brown (Elfar *et al.*, 2017). Lalève *et al.* (2014) reported that this fungus forms macroconidia for dispersal or sclerotia for survival, with its reproductive patterns being influenced by light exposure (Schumacher *et al.*, 2014). In vitro, the maximum development of its mycelium was observed within five days (Oztekin *et al.*, 2024), and the optimal growth temperature for *B. cinerea* ranges from 15-20°C (Ma *et al.*, 2018).

According to Damialis *et al.* (2015), the temperature was predicted to increase yearly and affect the phytopathogen population causing disease. The optimum temperature for *B. cinerea* growth was increased yearly which is in line with the climatic changes (Hegyi-Kaló *et al.*, 2019). This was due to the adaptation of the pathogen to the warmer temperatures and became more prevalent (Velásquez *et al.*, 2018). Regarding relative humidity, Ciliberti *et al.* (2015) found as the relative humidity (RH) increased, the disease incidence and severity of gray mold also increased but no disease incidence was observed at 65% of RH. To date, not much study has been done on *Botrytis*-incited tomato fruits in Malaysia. The incidence of this disease in tomatoes sampled from Cameron Highland was found in 2015 and reported by Tijjani *et al.* (2018). However, this pathogen was massively reported worldwide, especially in temperate countries, due to its disastrous impact on economic losses not only on tomatoes but hundreds of species of plants (Collinge & Sarrocco, 2022).

The morphological and genetic variation of each *Botrytis* species varies according to geographical area, season, fungicide treatment, and host plant. However, information on morphology, genetic study, and pathogenesis of *B. cinerea* isolated from tomatoes in Malaysia remains scarce. This information is crucial for developing effective disease management strategies for horticultural crops. Therefore, the goals of the present study were: (a) to isolate *Botrytis cinerea* causing gray mold disease on tomatoes; (b) to characterize the *Botrytis* isolates based on morphological and molecular identification using the internal transcribed spacer (ITS) region; and (c) to conduct a pathogenicity test.

MATERIALS AND METHODS

Sample collection

Twenty-one tomato fruits with gray mold were collected from the field of Cameron Highlands, Pahang (geographical coordinates: 4°30'24.4"N 101°24'48.0"E, Malaysia) in February 2018. The symptoms observed were necrotic tissue with the extensive growth of white to gray mycelium. Each of the symptomatic fruits was kept in a separate ziplock bag and immediately transported to the Pathology Laboratory.

Isolation of pathogen

The isolation of fungi pathogen has been conducted according to Yusoff *et al.* (2021), the edges of lesions on tomato fruits were dissected into pieces measuring 5 mm × 5 mm. These pieces were subjected to surface sterilization using a 70% (*v/v*) ethanol solution for 15 sec. Subsequently, they were rinsed twice with sterile distilled water for 1 min each. The excised tissues were blotted dry on sterilized filter paper and placed on potato dextrose agar, PDA (39 g/L), and kept in an incubator (Model LM-575RD, Taiwan) at 20°C under the illumination of fluorescent light and 12-hr photoperiod. The isolated culture was sub-cultured to obtain a pure culture. Cultures were examined every day for two weeks. Isolates were mounted on PDA slants at 4°C in the dark for longer-term storage.

Morphological characterization of *B. cinerea*

All *Botrytis* isolates on PDA were incubated at 5, 10, 15, 20, and 25°C, with three replicates per isolate per temperature treatment. After five days, the colony color at the upper and lower surfaces was observed, and the mycelial growth from the diameter in two perpendicular directions was measured. Sporulation of *B. cinerea* isolates was performed according to Petsikos-Panayotarou *et al.* (2003) protocols. Mycelial plugs (4-mm diameter) were excised from the colony edge and cultured on V-8-juice agar medium (containing 348 mL V8 juice and 20 g agar/L) and incubated at 20 ± 2°C for 8 days in the dark. The shape and size of the conidiophore (*n*=10/isolate) and conidia (*n*=40/isolate) were measured after 8 days of incubation. Sclerotia were produced on PDA at 20 ± 2°C and the shape and size of the sclerotia (*n*=10/isolate) were recorded after 3 to 5 weeks of incubation. Photographs were taken under a Dino-Lite digital microscope (AM4113TL-M40).

Molecular identification of *B. cinerea* using Ribosomal DNA Internal Transcribed Spacer (rDNA-ITS)

Fungal DNA extraction

An eight-day-old mature culture of each *Botrytis* isolate, grown on PDA agar at 20±2°C, was prepared for DNA extraction. Total DNA extraction was performed by using DNeasy® Plant Mini Kit (Qiagen, Hilden, Germany) (Cat. No. 69106) following the manufacturer's protocols. Approximately 1 g of each mycelial culture was scraped gently by scalpel blades and ground using mortar and pestle. The grounded mycelia were then transferred into a 1.5 mL microcentrifuge tube and added with 450 µL and 4 µL of buffer AP1 and RNase A. The mixture in microcentrifuge tubes was vortexed for about 15 sec until no clump of mycelial was observed. Next, the tubes were incubated for 10 min at 65°C in a digital dry bath (Labnet AccuBlock™ D1100, USA), with occasional inversion. After incubation, 150 µL of buffer P3 was added to the tubes and incubated in ice for 5 min.

The lysate was centrifuged at 14, 000 rpm for 5 min using an Eppendorf centrifuge (Model 54030R, Germany). The lysate was then transferred to a purple QIAshredder spin column in a 2-mL collection tube and centrifuged at 14,000 rpm for 2 min. The flow-through was carefully transferred to a new tube. Buffer AW1 at 1.5 volumes was added and mixed by pipetting. The resulting mixture, pipetted to a volume of 650 µL, was then transferred to a white DNeasy Mini spin column. This column was then positioned within a 2 mL collection tube and subjected to centrifugation at a speed of 8,000 revolutions per min for 1 min. The flow-through was disposed of. The aforementioned procedure was replicated with the remaining sample. Subsequently, the spin column was carefully inserted into a fresh 2 mL collection tube. A volume of 500 µL of Buffer AW2 was added, followed by centrifugation at a speed of 8,000 rpm for 1 min. The flow-through was disposed of. An additional buffer, AW2, was added at a volume of 500 µL and subjected to centrifugation at a speed of 14,000 rpm for 2 min. The spin column was transferred to a new 1.5 mL microcentrifuge tube. Buffer AE at 100 µL was added for elution and incubated for 5 min at ambient temperature before it was centrifuged at 8, 000 rpm for 1 min. The step was repeated and finally, the spin column was removed meticulously, leaving the extracted DNA in the microcentrifuge tube. The extracted DNA was kept at -20°C for further assessment. The DNA purity was evaluated by comparing absorbance ratios at 260 and 280 nm using NanoDrop™ 2000C spectrophotometer (Thermo Scientific, USA) range of 1.8 to 2.0 as suggested by Sambrook *et al.* (1989).

PCR amplification and sequence analysis

Amplification of the partial ribosomal DNA (rDNA) was performed with primer pair ITS5 (5'-GGAAGTAAAAGTCGTAACAAGG-3') and ITS4 (5'-TCCTCCGCTTATTGATATGC-3') (Tijjani, 2018). The 50-µL total reaction mixture contained 4 µL of primers, 25 µL REDiant 2X PCR master mix (Cat. No. BIO-5185-200, containing reaction buffer, 0.06 U/µL of *Taq* DNA polymerase, 3 mm of $MgCl_2$, 400µM of dNTPs), 2.0 µL of fungal DNA template and 19 µL of nuclease-free water. The reactions were performed in a Mastercycler® (Eppendorf Model Pro 384, Germany) using the following cycling parameters: initial denaturation at 95°C for 2 min, 35 cycles of denaturation at 95°C for 45 sec, annealing at 52°C for 30 sec, extension at 72°C for 90 sec and final extension at 72°C for 10 min. Amplification of the DNA amplification was observed by using 1% agarose gel (Sigma-Aldrich) with tris-borate-EDTA (TBE) buffer at 70V. The predicted size of the PCR result was determined using a 1 kb DNA ladder obtained from Promega, USA. The gels were imaged using a UV transillumination documentation system (Bio-Rad, USA). The PCR products of the amplified ITS were sequenced with DNA Analyzer (Applied Biosystems™ Model 3730xl, USA) by Apical Scientific Sdn. Bhd. All edited DNA sequences were provisionally identified using nucleotide BLAST searches (National Center for Biotechnology Information (NCBI), Bethesda, MD), https://www.ncbi.nlm.nih.gov.

Pathogenicity test

Preparation of inoculum and growth conditions

B. cinerea used in this study is routinely maintained on V8 agar (V-8 Agar is a medium consisting of eight types of vegetables including carrot, spinach, tomato, celery, parsley, beets, watercresses, and lettuce) for 8 days at 20°C under a 12-hr photoperiod at 20±2°C before spore collection. The fungal spores were collected through the process of overflowing the plates with a volume of 10 mL of sterilized distilled water. The spores were meticulously detached from the surface of the V8 medium using a sterile bent glass rod, and subsequently, the suspensions were filtered through four layers of sterile cheesecloth to exclude any mycelial presence. The concentration of the spore's suspension containing 1% Tween-80 was adjusted to 1 x 10^5 mL^{-1} using a Neubauer hemocytometer. A solution of distilled water with 1% Tween-80 without spores was used as the control treatment.

Pathogenicity test on detached tomato fruits

Pathogenicity assays were performed following the methodology outlined by Zhang *et al.* (2014), with slight adjustments made to the experimental protocol. A total of ten Botrytis isolates were employed to conduct pathogenicity and aggressiveness assessments on detached tomato fruits (var. Syngenta 1039) inside a controlled environment. Forty-four tomato fruits without visible disease were purchased from Weng Seng Vegetable Products Sdn. Bhd., Cameron Highland, Pahang, Malaysia. The fruits underwent surface sterilization by immersing them in a solution of 70% ethanol (*v/v*) for 1 min. Following this, the fruits were rinsed three times using distilled water that had been sterilized using autoclaving. Subsequently, the fruits were left to air-dry in a laminar flow environment at room temperature for 30 min.

A wounded depth of 4 mm was created using a sterile nail at the central cheek of each fruit and inoculated by pipetting 10-µL of conidial suspension (1 x 10^5/mL) on the wound. Four tomato fruits were inoculated with distilled water containing 1% Tween 20 served as a control treatment. The fruits that had been subjected to inoculation were placed in a plastic container and securely sealed within plastic bags. These bags were sprayed with water internally to ensure a consistently high level of humidity. The container, along with its enclosed fruits, was then incubated at a controlled temperature of 25 ± 2°C. (Figure 1). The pathogenicity test was repeated once. The lesion diameter (mm) on the inoculated fruits was measured daily for up to 5 days.

Fig. 1. Fruit storage condition after inoculation.

The disease severity was evaluated daily and grouped into five scales based on the fruits lesion described by Rosero-Hernández *et al.* (2019); 0 = no visible symptoms of fruits (no infection); 1 = 1-25% inoculated area covered with slight necrotic and water-soaked lesion (mild infection); 2 = 26-50% of the inoculated area covered with necrotic, white to grey mycelia and water-soaked lesion (moderate infection); 3 = 51-75% of fruits are necrotic with spore mass appeared and water-soaked (severe infection); and 4 = >76% necrotic tissue appears soft, watery and decay (very severe). The disease severity index (DSI) was calculated using the following equation:

$$DSI = \sum \frac{a \times n}{AB} \times 100$$

where a = disease scale, n = number of fruits in a specific scale, A = highest disease scale, B = total number of fruits.

Experimental design and statistical analysis

The study involved experimenting to observe the development of *B. cinerea* on PDA at various temperatures, as well as conducting a pathogenicity test. The experiment followed a completely randomized design (CRD) with four replications. The data underwent analysis of variance (ANOVA), and the means were differentiated using the least significant difference (LSD) test at a significance level of $p<0.05$. The data analysis was conducted using SAS software, specifically version 9.4.

RESULTS

Gray mold disease symptoms

The gray mold symptoms on tomato fruits sampled from Cameron Highlands showed rotted tissue with white and grayish mycelium that developed into soft, watery, and decay lesions covered with abundant conidia, as well as some black sclerotia (Figure 2).

Fig. 2. The presence of gray mold symptoms was seen on tomato fruits collected from Cameron Highlands.

Identified botrytis species based on morphological characteristics

Different growth patterns of *B. cinerea* were observed on PDA at 5, 10, 15, 20, and 25°C. The highest rapid growth of fungus was detected at 20°C, followed by 15°C and 10°C (Figure 3). In this study, the lowest temperature of 5°C has restricted the mycelial growth. Nevertheless, in vitro *B. cinerea* colony did not grow at all at 25°C.

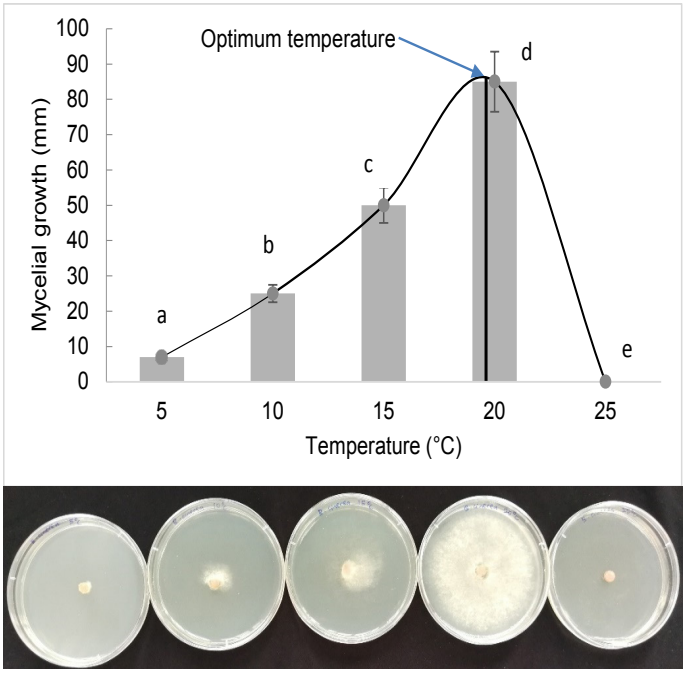

Fig. 3. Influence of temperature on the growth of mycelium in Botrytis cinerea, a fungal pathogen isolated from tomato fruits exhibiting signs of disease. Growth after 5 days on PDA. Means with the same letter are not significantly different at $p>0.05$ using the LSD test.

This study encompassed an examination of many morphological aspects of Botrytis species responsible for gray mold, including colony color, conidial form, measurements of colony development rate, and conidial length and width. Ten isolates were isolated and fungal isolates of *B. cinerea* initially produced white cottony colonies on 7-day-old cultures on PDA in both front and reverse views (Figure 4). The colonies progressively turned to gray mycelium covered with a few tiny whitish sclerotia after 3 weeks on PDA (Figure 5A) and became numerous after 4 weeks (Figure 5B). Large and irregular sclerotia with dark cortex developed after 5 weeks of incubation on PDA (Figure 5C). Sclerotia formed in scattered culture plates with spherical or irregular shapes.

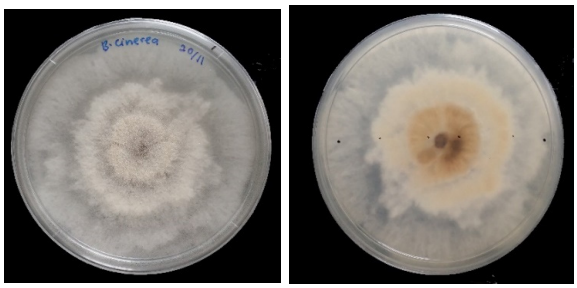

Fig.4 . The images presented depict the anterior view (left) and posterior view (right) of *Botrytis cinerea* full-grown on potato dextrose agar (PDA) medium following a 7-day incubation period.

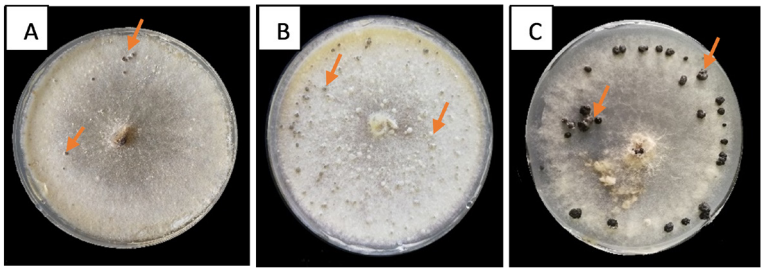

Fig. 5. The development of sclerotia in *Botrytis cinerea* isolates was seen on potato dextrose agar (PDA) medium. In (A), a culture that is three weeks old exhibits mycelium with a grayish hue and a limited presence of sclerotia formation. In (B), a culture that is four weeks old has little sclerotia that are whitish to grayish in colour, distributed around the surface of the PDA medium. In (C), a culture that is five weeks old demonstrates an increase in size and hardening of the sclerotia, which have turned black in colour.

The mycelium was branched, septate, hyaline, and brown (Figure 6A). Conidiophores were arising directly from the mycelia. They were single, smooth, terminally-branched, grayish, grape-shaped (Figure 6B). Conidiophores were straight, septate, branched, and pale brown. Conidia were hyaline, one-celled, ellipsoid, or ovoid (Figure 6C).

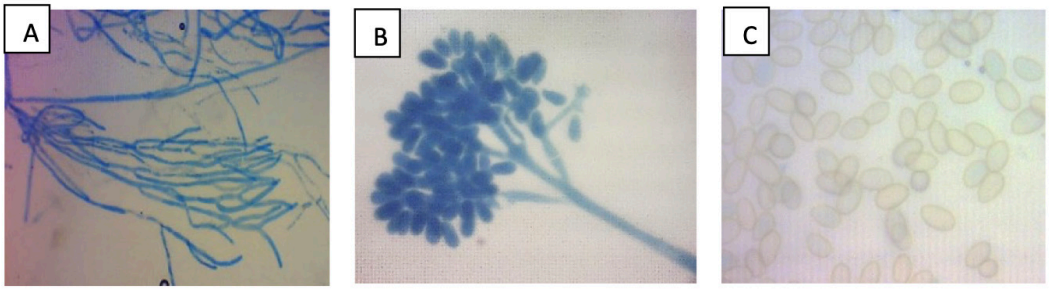

Fig. 6. Morphological characteristics of *Botrytis cinerea* are as follows. (A) The branched mycelium was observed under a light microscope at a magnification of 4x. (B) A conidiophore was observed producing blastoconidia at a magnification of 10x. (C) The conidia were observed at a magnification of 40x.

All ten isolates were denoted as P1 to P10. In terms of conidiophore size, it was ranged 21.26-32.52 µm, *n*=10. Among isolates, the minimum conidia size was P9 (10.03×9.76 µm, *n*=40) and the maximum conidia size was P2 (15.32×11.15 µm, *n*=40). Meanwhile, sclerotia appeared to vary in size from the smallest obtained from P1 isolate to the largest obtained from P7 isolate. The physical traits observed exhibit a resemblance to the documented description of *Botrytis cinerea* Pers. (Javed *et al.* 2017; Tijjani *et al.*, 2018).

Identified *B. cinerea* based on molecular identification

All ten isolates were denoted as P1 to P10 and compared for ITS sequence. A single band with a total size of 550 bp was obtained from the amplified isolates. BLAST analyses of the NCBI GenBank database with ITS region sequences of the pathogen cultures isolated from tomato fruit showed that the closest match (maximum identity 99-100%) was *Botrytis cinerea* (Table 1). The query coverage was 98 and 99% for ITS-rDNA.

Table 1. Identity of isolates based on ITS region comparison with nucleotide sequences from GenBank

Isolate	Fungi Species	Isolates Accession No.	Total Score	Query Coverage (%)	Identity (%)	Best Match Accession No.
P1	*B. cinerea*	MT012053	968	98	99.81	KX889115
P2	*B. cinerea*	MT012054	977	98	100.00	MH860108
P3	*B. cinerea*	MT012055	977	99	100.00	KR094468
P4	*B. cinerea*	MT012056	977	98	100.00	CP009808
P5	*B. cinerea*	MT012057	976	99	100.00	KF859918
P6	*B. cinerea*	MT012058	970	98	99.81	MK346204
P7	*B. cinerea*	MT012059	965	98	99.81	KX889115
P8	*B. cinerea*	MT012060	977	98	100.00	MH860108
P9	*B. cinerea*	MT012061	977	98	100.00	KJ744343
P10	*B. cinerea*	MT012062	977	98	100.00	MH860108

Pathogenicity assay

All ten isolates that were subjected to testing exhibited pathogenicity towards tomato fruits. There was a notable variation in the level of aggressiveness exhibited by the tested isolates on tomato fruits, as evidenced by the range of lesion sizes observed, which spanned from 1.75 cm to 5.83 cm (2). Based on the diameter sizes of the lesions, aggressiveness was classified as strongly virulent cause (>76% infected area), moderately virulent cause 26-75% infected area, or weakly virulent (<25% infected area). Among the 10 isolates investigated, P6 isolates were strongly virulent, followed by P8, P3, P1, P7, P5, P10, and P2 isolates were moderately virulent, P4 and P9 isolates were weakly virulent. The least virulent strain was the P9 isolate, while the most virulent strain was the P6 isolate.

Table 2. Aggressiveness of *B. cinerea* isolates on tomato plants after 5 days of inoculation, based on lesion width and disease severity

Species	Isolates	Lesion diameter (Mean±SE, cm)	Disease severity (Mean±SE, %)
B. cinerea	P1	3.25±0.31 c^{X}	48.51±4.62 c^{X}
B. cinerea	P2	2.58±0.09 d	38.43±1.27 d
B. cinerea	P3	4.03±0.25 b	60.08±3.77 b
B. cinerea	P4	1.65±0.13 e	24.63±1.97 e
B. cinerea	P5	3.00±0.20 cd	44.78±2.92 cd
B. cinerea	P6	5.55±0.06 a	82.84±0.96 a
B. cinerea	P7	3.25±0.39 c	48.51±5.86 c
B. cinerea	P8	4.55±0.10 b	67.91±1.55 b
B. cinerea	P9	1.45±0.06 e	21.64±0.96 e
B. cinerea	P10	2.95±0.10 cd	44.03±1.43 cd

Values are represented as mean ± SD. The groups denoted by ^{X}, which consist of identical letters within, do not exhibit statistically significant differences at a significance level of $p>0.05$ as determined by the LSD test.

Gray mold signs appeared on the inoculated fruits after three days, while the control fruits did not exhibit any symptoms. The disease severity gradually increased when the fruits were incubated longer time (Figure 7). The initial symptom appeared as a translucent bruise at the inoculation site. The infected area developed soft, watery, and whitish mycelium that became visible after 3 days of incubation. The lesion rapidly expanded on the surface of the fruits showing severe symptoms after 4 days incubation. On the final day of fruit storage, the mycelium turned to a fuzzy gray-brown, water-soaked lesion, the lesion more than half of the fruit surface, and a strong sour-rot smell. However, the control fruits have remained symptomless. The pathogenicity test was carried out twice with similar results. The pathogen was successfully reisolated from the lesions of inoculated fruits, fulfilling Koch's postulates. Similar morphological characteristics were found when compared with the original isolates.

The highest pathogenic level of P6 isolate on artificial inoculated tomato fruits was pictured in Figure 8A-C. The necrotic lesion was very severe with more than 76% fruit surface covered with white to gray mycelium. The fruit tissue was also soft and watery. Moderate pathogenic symptoms of P8, P3, P1, P7, P5, P10, and P2 were observed in Figure 8D-I with the lesion covering 26-50% of the fruits. Figure 8J-K indicated less pathogenic of P4 and P9 and the fruit symptoms were slightly necrotic ranged 1-25%. No disease symptoms were detected on control fruits, as shown in Figure 8L.

Fig. 7. The manifestation of gray mold disease symptoms on tomato fruits occurs between the second and fifth days following inoculation with spores of *Botrytis cinerea*.

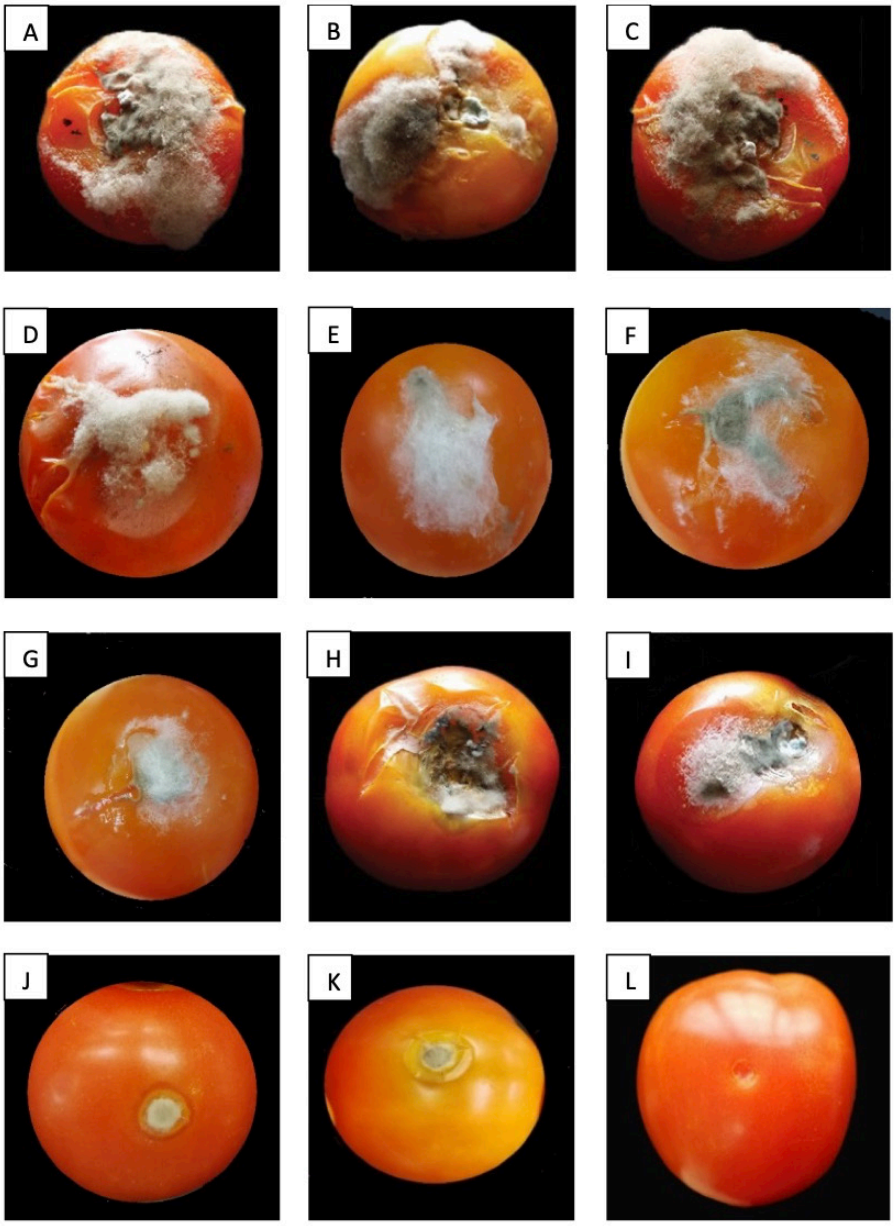

Fig. 8. Disease severity levels of *B. cinerea* isolates on artificially inoculated tomato. (A to C) Highly pathogenic; (D to I) Moderately pathogenic; (J & K) Mild Pathogenic; and (L) Symptomless on control fruits after 5 days of inoculation.

DISCUSSION

The present study found that 20°C was the optimum and the most conducive growth for *B. cinerea* isolated from tomatoes in Cameron Highlands, Malaysia. This finding was consistent with Hegyi-Kaló *et al.* (2019) who reported that 20°C was the highest growth rate of *B. cinerea* but the growth rate decreased at 15 and 25°C after 4 days of post-inoculation. The present results also confirmed the model developed by Judet-Correia *et al.* (2010) in predicting temperature effects on the mycelial growth

rate of *B. cinerea*. Agrios (2005) stated that tomato fruits are susceptible to being infected by *B. cinerea* at low-temperature conditions ranged 18-23°C. Some researchers reported this pathogen can infect fresh produce and disperse their conidia even stored at -0.5°C (Crisosto *et al.*, 2002). In contrast, some of the *B. cinerea* isolates were able to grow at 25°C (Tijjani *et al.*, 2018).

In this study, there was no specific pattern variation in colony growth, color, or morphological features such as conidiophores, conidia, and sclerotia among *B. cinerea* isolates. Based on macroscopic and microscopic examination, the morphological characteristics were similar to *B. cinerea* as described by Tijjani *et al.* (2018) and Javed *et al.* (2017). The colony from the isolates became darker as the age of the fungal cultures increased. The same observation was reported by Ma *et al.* (2018), who justified that at this stage, the mycelium almost stopped growing and became aging. Cantu *et al.* (2009) reported the mycelium age of *B. cinerea* affected not only the color appearance but also cell wall composition due to diminishing nutrient supply.

In terms of conidia size, the average length and width ranged from 10.03-16.08 × 9.01-11.15 µm, respectively. Other researchers found the average conidia size of *B. cinerea* isolated from tomatoes was 9.7-17.1 × 6.6-10.5 µm. The size of conidia of *B. cinerea* was varied from different hosts such as sponge gourd was 5.8–10.2 × 4.8–7.2 µm (Aktaruzzaman *et al.*, 2016), carrot was 6.3-11.8 × 5.2-8.0 µm (Aktaruzzaman *et al.*, 2014), broccoli was 5.3-10.1 × 4.3-9.3 µm (Aktaruzzaman *et al.*, 2017), okra was 4.2-9.8 × 3.9-8.2 (Afroz *et al.*, 2019) and rose flower was 4.0-13.0 × 2.0-7.0 µm (Khazaeli *et al.*, 2010). Generally, conidia appeared in micrometer size and abundance on the infected fruit's surface. Due to their size, lightweight, and abundant amount, conidia of *B. cinerea* were considered as a primary dispersed inoculum (Fillinger & Elad, 2016). The asexual spores possessed the capacity to be spread through either wind or water. Thus, appropriate measures and handling should be implemented at every possible entry point either pre-harvest or postharvest stage. A standard postharvest practice also should be mandatorily implemented to minimize the fruit's infection such as isolating the infected fruits with the healthy fruits at the sorting stage, treating the fruits with disinfection treatment before being packed, and sanitizing the equipment and cold room periodically.

The present study found sclerotia came out in hard, black, and millimeter sizes that can be noticed by the naked eye. Other scientists also found distinct sclerotia sizes subjected to their shape and arrangement either in a circle, irregular, scattered, or edge of the petri dish (Tanovic *et al.*, 2015). Sclerotia is composed of compacted masses of mycelia. It is a resting structure that helps this pathogen to survive under adverse circumstances for example UV irradiation, high or low temperatures especially during winter, desiccation, and other microbial attacks (Zhou *et al.*, 2018). This unique structure could be found in soil, plant debris, stems, and rotten fruits in the field (Holz *et al.*, 2007). *Botrytis* sclerotia was considered a long-term dormant structure because it could survive at least 18 months without a host and only germinated when favorable condition was obtained (Hsiang & Chastagner, 1992). Sclerotia is composed of cortex cells and appears in a dark color, especially at the outer layer.

Molecular identification was carried out to support morphological characteristics observation. In the current study, the ITS region of rDNA isolates was amplified and sequenced using ITS5/ITS4 primers. The results of all isolates from BLAST analysis of 550-bp nucleotide sequences based on ITS region presented the gene alignment was 99-100% matched to *Botrytis cinerea*. Similar results were declared by other pathologists using the same type of ITS primers (Javed *et al.*, 2017; Afroz *et al.*, 2019). However, the sample size and collection in this study might not represent the frequency distribution in Malaysia as the sample was only in Cameron Highland.

Koch's postulates confirmed that all 10 isolates were *B. cinerea*. The outcomes from pathogenicity experiments revealed these 10 isolates of *B. cinerea* were pathogenic and caused gray mold development. However, the pathogenicity and virulence behavior of each isolate were varied during the incubation period. This variation is probably due to the conidial ability to germinate, competency to colonize the host, and establish the lesion on the fruit surface (Schumacher & Tudzynski, 2012; Bojkov *et al.*, 2019). P6 isolate showed the most virulent pathogen that aggressively ruptured the fruit tissue and caused ionic leakage. The severity level of fruits was increased after a few days of fruit infection with the highest pathogenic level achieved after 5 days of inoculation. According to Derckel *et al.* (1999), the aggressiveness level of *B. cinerea* isolates was associated with cell wall degrading enzyme capacity and oxalic acid accumulation. Besides, tomato being a delicate fruit was prone to physical injury that hastened the severity level of *B. cinerea* infection. These were observed from the lesion area at the artificial inoculation of wounded fruit in this study. Fillinger and Elad (2016) stated that the opening cut, bruising, and abrasion on the fruit's surface led to the entry point of *B. cinerea* colonization and sped the infection.

CONCLUSION

Pathological damage on fruits at the postharvest stage is a prominent issue about food quality and safety as well as economic loss. Based on mycological characteristics, molecular data, symptoms appearance, and pathogenicity assays, the isolates from the tomato fruits in Cameron Highlands were identified as *Botrytis cinerea*. The typical disease symptoms of gray mold disease were seen on the third day of infection. The infected area was soft and water-soaked with the presence of white mycelium. The primary results of this study are very important to verify the pathogen involved in gray mold disease on tomato Cameron Highlands for outlining an accurate disease management strategy.

ACKNOWLEDGEMENTS

The authors acknowledged the Ministry of Higher Education (MoHE) Malaysia for supporting this project through the Fundamental Research Grant Scheme (FRGS/1/2015/WAB01/UPM/02/5).

ETHICAL STATEMENT

Not applicable.

CONFLICT OF INTEREST

The authors declare no conflict of interest.

REFERENCES

Afroz, T., Aktaruzzaman, M. & Kim, B.S. 2019. First report of gray mold on okra caused by *Botrytis cinerea* in Korea. Plant Disease, 103(5): 1038-1038. https://doi.org/10.1094/PDIS-10-18-1884-PDN

Agrios G.N. 2005. Plant Pathology, 5th Ed. Academic Press, California.

Aktaruzzaman, M., Afroz, T., Hong, S.J. & Kim, B.S. 2017. Identification of *Botrytis cinerea*, the cause of post-harvest gray mold on broccoli in Korea. Research in Plant Disease, 23(4): 372-378. https://doi.org/10.5423/RPD.2017.23.4.372

Aktaruzzaman, M., Afroz, T., Kim, B.S. & Shin, H.D. 2016. First report of gray mold disease of sponge gourd (*Luffa cylindrica*) caused by *Botrytis cinerea* in Korea. Research in Plant Disease, 22(2): 107-110. https://doi.org/10.5423/RPD.2016.22.2.107

Aktaruzzaman, M., Kim, J.Y., Xu, S.J. & Kim, B.S. 2014. First report of postharvest gray mold rot on carrot caused by *Botrytis cinerea* in Korea. Research in Plant Disease, 20(2): 129-131. https://doi.org/10.5423/RPD.2014.20.2.129

Bautista-Baños, S. 2014. Postharvest Decay: Control Strategies. Elsevier. 383 pp. https://doi.org/10.1016/B978-0-12-411552-1.00001-6

Bojkov, G., Mitrev, S. & Arsov, E. 2019. Impact of ampelotechnical measures in the grapevine protection from occurrence of grey mould (*Botrytis cinerea*). Journal of Animal and Plant Sciences, 17(1): 29-41.

Cantu, D., Blanco-Ulate, B., Yang, L., Labavitch, J.M., Bennett, A.B. & Powell, A.L.T. 2009. Ripening-regulated susceptibility of tomato fruit to *Botrytis cinerea* requires NOR but not RIN or ethylene. Plant Physiology, 150(3): 1434-1449. https://doi.org/10.1104/pp.109.138701

Ciliberti, N., Fermaud, M., Roudet, J. & Rossi, V. 2015. Environmental conditions affect *Botrytis cinerea* infection of mature grape berries more than the strain or transposon genotype. Phytopathology, 105(8): 1090-1096. https://doi.org/10.1094/PHYTO-10-14-0264-R

Collinge, D. B. & Sarrocco, S. 2022. Transgenic approaches for plant disease control: Status and prospects 2021. Plant Pathology, 71(1): 207-225. https://doi.org/10.1111/ppa.13443

Crisosto, C.H., Garner, D. & Crisosto, G. 2002. Carbon dioxide-enriched atmospheres during cold storage limit losses from *Botrytis* but accelerate rachis browning of 'Redglobe' table grapes. Postharvest Biology and Technology, 26(2): 181-189. https://doi.org/10.1016/S0925-5214(02)00013-3

Damialis, A., Mohammad, A.B., Halley, J.M. & Gange, A.C. 2015. Fungi in a changing world: Growth rates will be elevated, but spore production may decrease in future climates. International Journal of Biometeorology, 59(9): 1157-1167. https://doi.org/10.1007/s00484-014-0927-0

Derckel, J.P., Baillieul, F., Manteau, S., Audran, J.C., Haye, B., Lambert, B. & Legendre, L. 1999. Differential induction of grapevine defenses by two strains of *Botrytis cinerea*. Phytopathology, 89(3): 197-203. https://doi.org/10.1094/PHYTO.1999.89.3.197

Elfar, K., Riquelme, D., Zoffoli, J.P. & Latorre, B.A. 2017. First report of *Botrytis prunorum* causing fruit rot on kiwifruit in Chile. Plant Disease, 101(2): 1-388. https://doi.org/10.1094/PDIS-05-16-0775-PDN

Fillinger, S. & Walker, A.S. 2016. Chemical control and resistance management of *Botrytis* diseases. In S. Fillinger & Y. Elad (Eds.), *Botrytis*-The fungus, the pathogen and its management in agricultural

systems. Springer. 189-216 pp. https://doi.org/10.1007/978-3-319-23371-0_10

Hegyi-Kaló, J., Holb, I.J., Lengyel, S., Juhász, Á. & Váczy, K.Z. 2019. Effect of year, sampling month and grape cultivar on noble rot incidence, mycelial growth rate and morphological type of *Botrytis cinerea* during noble rot development. European Journal of Plant Pathology, 155: 339-348. https://doi.org/10.1007/s10658-019-01745-8

Holz, G., Coertze, S. & Williamson, B. 2007. The ecology of *Botrytis* on plant surface. In Y. Elad; B. Williamson; P. Tudzynski & N. Delen (Eds.), Botrytis: Biology, Pathology and Control. Springer. 9-27 pp. https://doi.org/10.1007/978-1-4020-2626-3_2

Hsiang, T. & Chastagner, G.A. 1992. Production and viability of sclerotia from fungicide-resistant and fungicide-sensitive isolates of *Botrytis cinerea*, *B. elliptica* and *B. tulipae*. Plant Pathology, 41(5): 600-605. https://doi.org/10.1111/j.1365-3059.1992.tb02459.x

Javed, S., Javaid, A., Anwar, W., Majeed, R.A., Akhtar, R. & Naqvi, S.F. 2017. First report of *Botrytis* bunch rot of grapes caused by *Botrytis cinerea* in Pakistan. Plant Disease, 101(6): 1036. https://doi.org/10.1094/PDIS-05-16-0762-PDN

Judet-Correia, D., Bollaert, S., Duquenne, A., Charpentier, C., Bensoussan, M. & Dantigny, P. 2010. Validation of a predictive model for the growth of *Botrytis cinerea* and *Penicillium expansum* on grape berries. International Journal of Food Microbiology, 142(1-2): 106-113. https://doi.org/10.1016/j.ijfoodmicro.2010.06.009

Khazaeli, P., Zamanizadeh, H., Morid, B. & Bayat, H. 2010. Morphological and molecular identification of *Botrytis cinerea* causal agent of gray mold in rose greenhouses in central regions of Iran. International Journal of Agricultural Science, 1(1): 19-24.

Lalève, A., Fillinger, S. & Walker, A.S. 2014. Fitness measurement reveals contrasting costs in homologous recombinant mutants of *Botrytis cinerea* resistant to succinate dehydrogenase inhibitors. Fungal Genetics and Biology, 67: 24-36. https://doi.org/10.1016/j.fgb.2014.03.006

Leyronas, C., Duffaud, M., Parès, L., Jeannequin, B. & Nicot, P.C. 2015. Flow of *Botrytis cinerea* inoculum between lettuce crop and soil. Plant Pathology, 64(3): 701-708. https://doi.org/10.1111/ppa.12284

Ma, S., Hu, Y., Liu, S., Sun, J., Irfan, M., Chen, L.J. & Zhang, L. 2018. Isolation, identification and the biological characterization of *Botrytis cinerea*. International Journal of Agricultural and Biological Engineering, 20(5): 1033-1040.

Oztekin, S., & Karbancioglu-Guler, F. 2024. Recruiting grape-isolated antagonistic yeasts for the sustainable bio-management of *Botrytis cinerea* on grapes. Food and Energy Security, 13(1): e528. https://doi.org/10.1002/fes3.528

Petsikos-Panayotarou, N., Markellou, E., Kalamarakis, A.E., Kyriakopoulou, D. & Malathrakis, N.E. 2003. In vitro and in vivo activity of cyprodinil and pyrimethanil on *Botrytis cinerea* isolates resistant to other botryticides and selection for resistance to pyrimethanil in a greenhouse population in Greece. European Journal of Plant Pathology,109(2): 173-182. https://doi.org/10.1023/A:1022522420919

Rosero-Hernández, E.D., Moraga, J., Collado, I.G. & Echeverri, F. 2019. Natural Compounds That modulate the development of the fungus *Botrytis cinerea* and protect *Solanum lycopersicum*. Plants, 8(5): 111. https://doi.org/10.3390/plants8050111

Sambrook, J., Fritsch, E.F. & Maniatis, T. 1989. Molecular cloning: A laboratory manual, second Ed. Cold Spring Harbor Laboratory Press (CSH Press).

Schumacher, J. & Tudzynski, P. 2012. Morphogenesis and infection in *Botrytis cinerea*. In: Morphogenesis and Pathogenicity in Fungi. J.P Martin and A. Di Pietro (Eds.). Springer. Place of publication. 225-241 pp. https://doi.org/10.1007/978-3-642-22916-9_11

Schumacher, J., Simon, A., Cohrs, K.C., Viaud, M. & Tudzynski, P. 2014. The transcription factor BcLTF1 regulates virulence and light responses in the necrotrophic plant pathogen *Botrytis cinerea*. PLoS Genetics, 10(1): 1-21. https://doi.org/10.1371/journal.pgen.1004040

Tanović, B., Hrustić, J., Mihajlović, M., Grahovac, M. & Delibašić, G. 2014. *Botrytis cinerea* in raspberry in Serbia I: Morphological and molecular characterization. Pesticidi i Fitomedicina, 29(4): 237-247. https://doi.org/10.2298/PIF1404237T

Tijjani, A., Ismail, S.I., Khairulmazmi, A. & Dzolkhifli, O. 2018. First report of gray mold rot disease on tomato (*Solanum lycopersicum* L.) caused by *Botrytis cinerea* in Malaysia. Journal of Plant Pathology, 101(1): 207. https://doi.org/10.1007/s42161-018-0155-2

Velásquez, A.C., Castroverde, C.D.M. & He, S.Y. 2018. Plant-pathogen warfare under changing climate conditions. Current Biology, 28(10): 619-634. https://doi.org/10.1016/j.cub.2018.03.054

Yusoff, S.F., Haron, F.F., Asib, N., Mohamed, M.T.M. & Ismail, S.I. 2021. Development of *Vernonia amygdalina* leaf extract emulsion formulations in controlling gray mold disease on tomato

(*Lycopersicon esculentum* Mill.). Agronomy, 11: 373. https://doi.org/10.3390/agronomy11020373

Zhang, Z., Qin, G., Li, B. & Tian, S. 2014. Knocking out Bcsas1 in *Botrytis cinerea* impacts growth, development, and secretion of extracellular proteins, which decreases virulence. Molecular Plant-Microbe Interactions, 27(6): 590-600. https://doi.org/10.1094/MPMI-10-13-0314-R

Zhou, Y., Li, N., Yang, J., Yang, L., Wu, M., Chen, W. & Zhang, J. 2018. Contrast between orange and black colored sclerotial isolates of *Botrytis cinerea*: Melanogenesis and ecological fitness. Plant Disease, 102(2): 428-436. https://doi.org/10.1094/PDIS-11-16-1663-RE